

Realization of a scenario with two relaxation rates in the Hubbard Falicov-Kimball model

H. Barman,^{*} M. S. Laad,[†] and S. R. Hassan[‡]

Institute of Mathematical Sciences, Taramani, Chennai 600113, India



(Received 23 January 2017; published 15 February 2018)

A single transport relaxation rate governs the decay of both longitudinal and Hall currents in Landau Fermi liquids (FL). Breakdown of this fundamental feature, first observed in two-dimensional cuprates and subsequently in other three-dimensional correlated systems close to the Mott metal-insulator transition, played a pivotal role in emergence of a non-FL (NFL) paradigm in higher dimensions $D(>1)$. Motivated hereby, we explore the emergence of this “two relaxation rates” scenario in the Hubbard Falicov-Kimball model (HFKM) using the dynamical mean-field theory (DMFT). Specializing to $D = 3$, we find, beyond a critical Falicov-Kimball (FK) interaction, that two distinct relaxation rates governing distinct temperature (T) dependence of the longitudinal and Hall currents naturally emerges in the NFL metal. Our results show good accord with the experiment in $V_{2-y}O_3$ near the metal-to-insulator transition (MIT). We rationalize this surprising finding by an analytical analysis of the structure of charge and spin Hamiltonians in the underlying impurity problem, specifically through a bosonization method applied to the Wolff model and connecting it to the x-ray edge problem.

DOI: [10.1103/PhysRevB.97.075133](https://doi.org/10.1103/PhysRevB.97.075133)

I. INTRODUCTION

It is well known that a single transport relaxation rate governs the decay of both longitudinal and Hall currents in a Landau Fermi liquid (FL) metal. This is obviously related to the fact that both result from scattering processes involving the same Landau quasiparticle, carrying the quantum numbers of an electron. Observation of distinct relaxation rates in dc resistivity (ρ_{dc}) and Hall angle (θ_H) [1] data for cuprates led to a paradigm shift in the traditional view of strongly correlated electrons in metals in dimension $D > 1$. While such anomalous behavior can be rationalized in $D = 1$ Luttinger liquids (LL) by appealing to fractionalization of an electron into a neutral spinon and a spinless holon, the specific nature of electronic processes leading to the emergence of such features in $D > 1$ is an enigma. In fact, Anderson [2] predicted such a feature from a generalized “tomographic” LL state in $D = 2$, by hypothesizing spin-charge separation: $\rho_{dc}(T) \simeq T$ arose from holon-spinon scattering, while $\cot\theta_H(T) \simeq T^2$ emerged from spinon-spinon scattering. Though very attractive, a derivation of such a higher D LL-like state remains an open and unsolved issue of great current interest.

Surprisingly, subsequent experiments revealed similar “two relaxation rates” in $D = 3$ correlated systems as well. Specifically, simultaneous resistivity and Hall measurements in the classic Mott system $V_{2-y}O_3$ revealed the following: in the lightly doped ($0 < y \ll 1$) case, (i) the dc resistivity, $\rho_{dc}(T) = \rho(y) + AT^{\eta(y)}$, with $\eta(y)$ varies between 1.5 and 2, while the Hall angle’s cotangent, $\cot\theta_H \simeq C_1(y) + C_2(y)T^2$ for all $T > T_N$, the Néel ordering temperature [3,4]. This is an example of a $D = 3$ correlated metallic system exhibiting “two” relaxation rates. Later in ruthenates [5,6] and heavy fermionic materials

[7] similar behavior also has been noticed. These observations show that such features are not unique to $D = 2$ systems, but generic to metallic states on the border of the Mott metal-to-insulator transition (MIT). It is also interesting that disorder seems to be a very relevant perturbation in $V_{2-y}O_3$: The resistivity is well accounted for by a variable-range hopping form, attesting to the importance of disorder near the Mott transition [8]. In multiorbital $CaRuO_3$ and $YbRh_2Si_2$, orbital-selective physics generically leads to extinction of FL metallicity via “Kondo breakdown” and onset of “spin freezing” [5,9], wherein one would expect low-energy charge dynamics to be controlled by the (strong) “intrinsic disorder” scattering between the quasi-itinerant and effectively Mott localized components of the full one-particle spectral function (though, strictly speaking, consideration of $YbRh_2Si_2$ would require a multiband periodic Anderson model). The actual Mott transition in V_2O_3 is by now also established to involve multiorbital correlations and orbital-selective localization: in LDA+DMFT studies [10–13], the e_g^π states remain Mott localized, while the a_{1g} states remain bad metallic in the bad metal close to the MIT. In the quantum paramagnetic state where the Mott transition occurs, one may view the e_g^π states as an “intrinsic disorder,” providing a strong scattering channel for the a_{1g} carriers. Thus, it seems that the anomalous two-relaxation times are linked to the breakdown of FL metallicity arising from strong scattering processes involving either intrinsic scattering channels or extrinsic disorder close to the MIT.

II. MODEL AND METHOD

Motivated by these observations, we introduce a Hubbard Falicov-Kimball model (HFKM) in standard notations

$$\begin{aligned}
 H^{\text{HFKM}} = & -t \sum_{\langle i,j \rangle, \sigma} (c_{i\sigma}^\dagger c_{j\sigma} + \text{H.c.}) - \mu \sum_{i\sigma} (\hat{n}_{i\sigma}^c + \hat{n}_i^d) \\
 & + U \sum_i \hat{n}_i^c \hat{n}_i^d + U_{cd} \sum_{i,\sigma} \hat{n}_{i\sigma}^c \hat{n}_i^d
 \end{aligned} \quad (1)$$

^{*}hbarhbar@gmail.com

[†]mslaad@imsc.res.in

[‡]shassan@imsc.res.in

as an *effective* model that captures the interplay between itinerancy (t) and strong electronic correlations (Hubbard interaction U) and intrinsic or extrinsic (Falicov Kimball interaction U_{cd}) disorder scattering, μ being the chemical potential. Qualitatively, (i) U_{cd} can mimic an effectively Mott-localized band in an orbital-selective Mott transition (OSMT) scenario [10,11], or (ii) $U_{cd}n_i^d$ ($n_i^d \equiv \langle \hat{n}_i^d \rangle$) can also be viewed as an extrinsic disorder potential experienced by the correlated c fermions (in $V_{2-y}O_3$, one can regard this as disorder arising from a concentration y of V vacancies in the host system) [8]. The Falicov-Kimball (FK) model (Eq. (1) without Hubbard U term) has been widely studied where it is found that increasing U_{cd} leads to a MIT where the metallic (M) phase is a non-Fermi liquid (NFL) [14,15]. OSMT can occur in the presence or absence of Hund's coupling (when hopping varies in different orbitals) [16] and it has been found that the effective two orbital Hamiltonian with Hund's coupling reduces to the FK Hamiltonian when there is no spin flip or pair hopping term, resulting in a NFL physics [17].

This sets up a motivation to investigate how FL and NFL metallic phases compete, due to the interplay of the FK and Hubbard interactions, in the transport properties. We solve H^{HFKM} using the dynamical mean-field theory (DMFT) with iterated perturbation theory (IPT) as the solver for the effective impurity problem [18,19]. IPT is a second order perturbation approximation around the Hartree Fock self-energy, which satisfies both the atomic limit ($t = 0$) and weak-coupling limit ($U = 0$). Hence it acts as a scheme to capture the physics at moderate U/t , “interpolating” the two limits. Despite being an approximation, IPT has shown remarkable agreement with exact diagonalization (ED) and quantum Monte Carlo results on the single and multi-band Hubbard models [20,21]. Being easy-to-implement (no analytical continuation required since quantities are evaluated directly on real frequency axis). IPT has become a popular quantum impurity solver to gain a quick insight of a correlated lattice problem [19]. In our method, U_{cd} is treated as site-diagonal disorder within the coherent potential approximation (CPA) [22–24] at half filling with disorder concentration x between 0.4 to 0.5, using a semicircular band density of states for the c electrons as an approximation to the actual $D = 3$ system (it keeps the correct energy dependence near the band edges in $D = 3$). Within DMFT, it is long known that a correlated FL metal for small U_{cd} smoothly goes over to an incoherent bad metal without FL quasiparticles as U_{cd} increases [22]. Motivated by the fact that the two-relaxation times seem to be linked to proximity to the (pure or selective) Mott transition, we focus on the evolution of the (magneto)transport when U_{cd} is cranked up in the regime where $U/t = 3.3$ is chosen to be close to the critical $(U/t)_c \simeq 3.4$ where a purely correlation-driven Mott transition occurs [18]. A short discussion of the relevant DMFT formalism and the associated equations, adapted from Ref. [22] in the related context of a binary-alloy disordered Hubbard model, has been provided in Appendix A.

III. RESULTS AND DISCUSSION

In Fig. 1, we exhibit the dc resistivity $\rho_{dc}(T, U_{cd})$ for different U_{cd} and fixed $U/t = 3.3$ as a function of T . Several features stand out clearly: a correlated FL up to small $U_{cd} < 0.2U$,

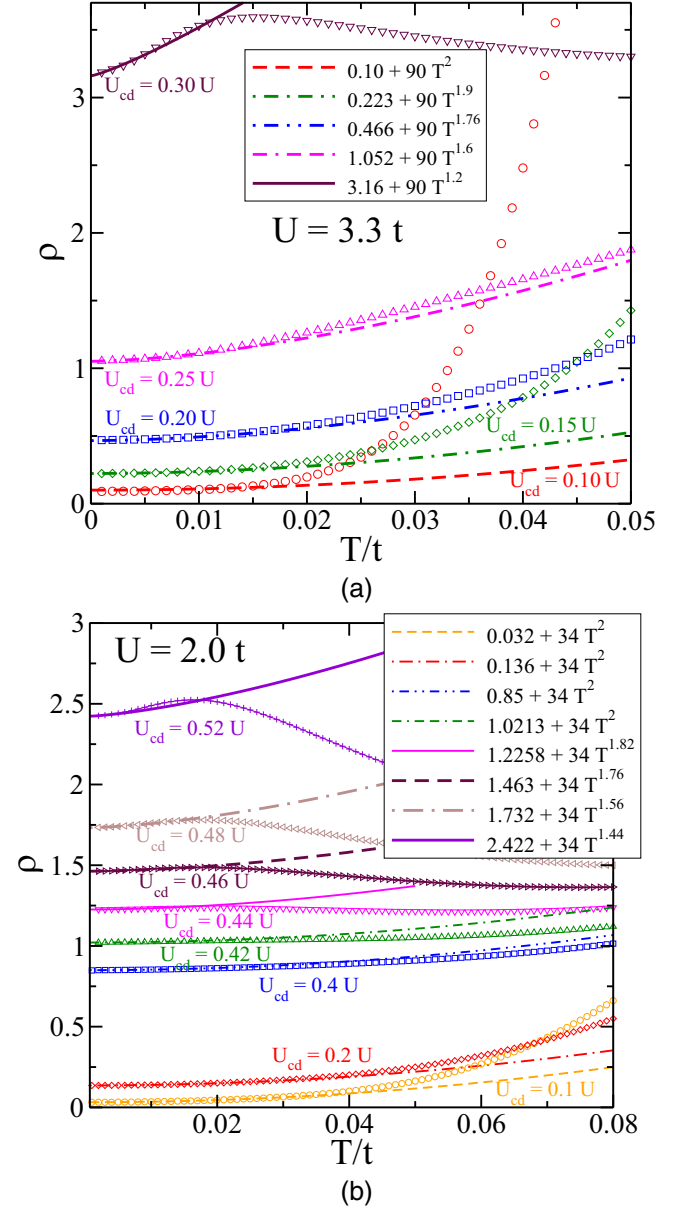


FIG. 1. DC resistivity vs temperature plot at (a) $U = 3.3t$ and (b) $U = 2.0t$. Dashed lines are power-law fits at low T .

where $\rho_{dc} = \rho_0(U, U_{cd}) + A(U)T^2$, smoothly evolves into an incoherent metal for $U_{cd} = 0.2U$, where we find $\rho_{dc}(T) = \rho_0 + AT^\alpha$, with $\alpha = 1.76$. It is very interesting that α seems to vary continuously with U_{cd} , ($\alpha = 1.6$ for $U_{cd} = 0.25U$, $\alpha = 1.2$ for $U_{cd} = 0.3U$), and the fact that ρ_{dc} remains bad metallic at intermediate-to-low T , crossing over to an insulatorlike form at high T for $U_{cd} = 0.3U$. Repeating the calculations for smaller $U/t = 2.0$, we find that while qualitatively similar features retain, $\rho_{dc}(T \rightarrow 0)$ rises to much higher values when U_{cd} is cranked up. This testifies to the increasing relevance of the strong scattering (from localized channels or extrinsic disorder as above) when U/t is in the weak-to-intermediate coupling regime. Since transport properties in DMFT do not involve vertex corrections in the Bethe-Salpeter equations for the conductivities, these features must be tied to loss of the FL quasiparticle pole structure in the DMFT one-electron

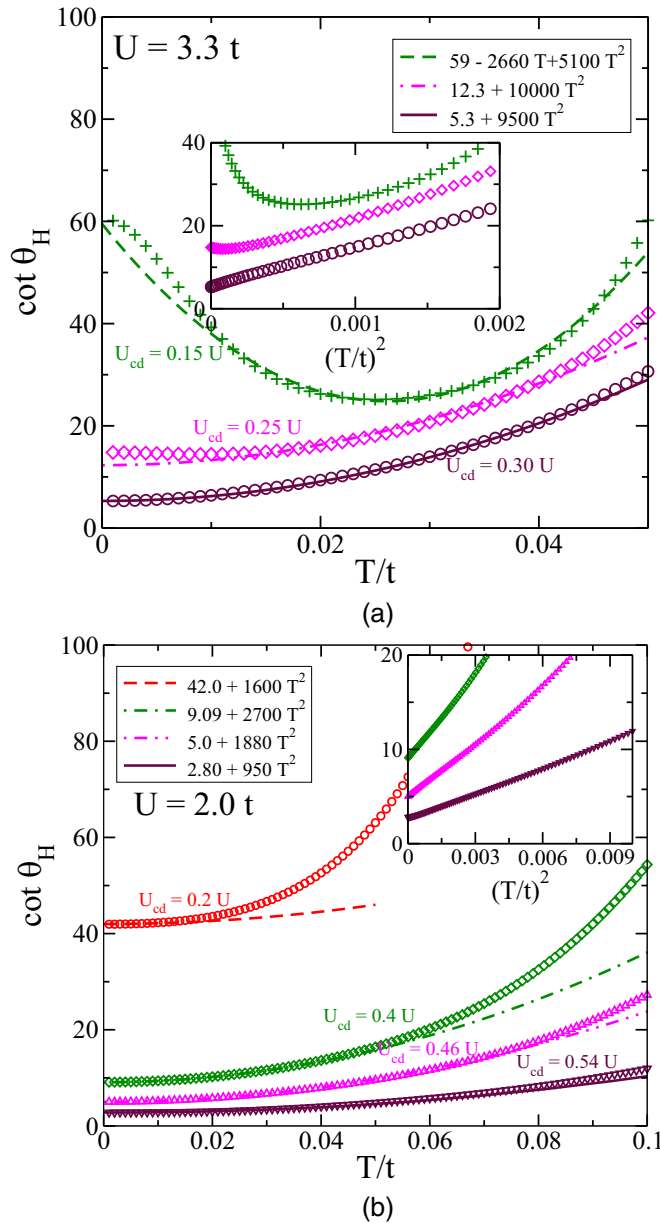


FIG. 2. Cotangent of Hall angle (θ_H) vs temperature plot at (a) $U = 3.3t$ and (b) $U = 2.0t$. Dashed lines are power-law fits at low T . Insets show the same against T^2 .

propagator, which is now the sole input to the renormalized bubble diagram for the conductivities [18].

Upon evaluating the off-diagonal conductivity (to first order in the vector potential \mathbf{A} as done before [25]) for H^{HFKM} in DMFT, we have computed the Hall constant (R_H) and Hall angle ($\cot \theta_H$) for the same parameter values as above. Even more remarkably, we find (see Fig. 2) that $\cot \theta_H \simeq C_1 + C_2 T^2$, up to $T/t = 0.05$ for both $U_{cd}/U = 0.25, 0.3$, while R_H exhibits a strong T dependence right down to the lowest T (see Fig. 3). This is the same parameter regime where $\rho_{dc}(T)$ exhibits NFL T dependence, with a U_{cd} -dependent exponent $1.0 < \alpha < 2.0$. Thus, our DMFT results directly reveal two-relaxation rates, and it is indeed notable that $\cot \theta_H \simeq C_1 + C_2 T^2$ continues to hold over a wide T range,

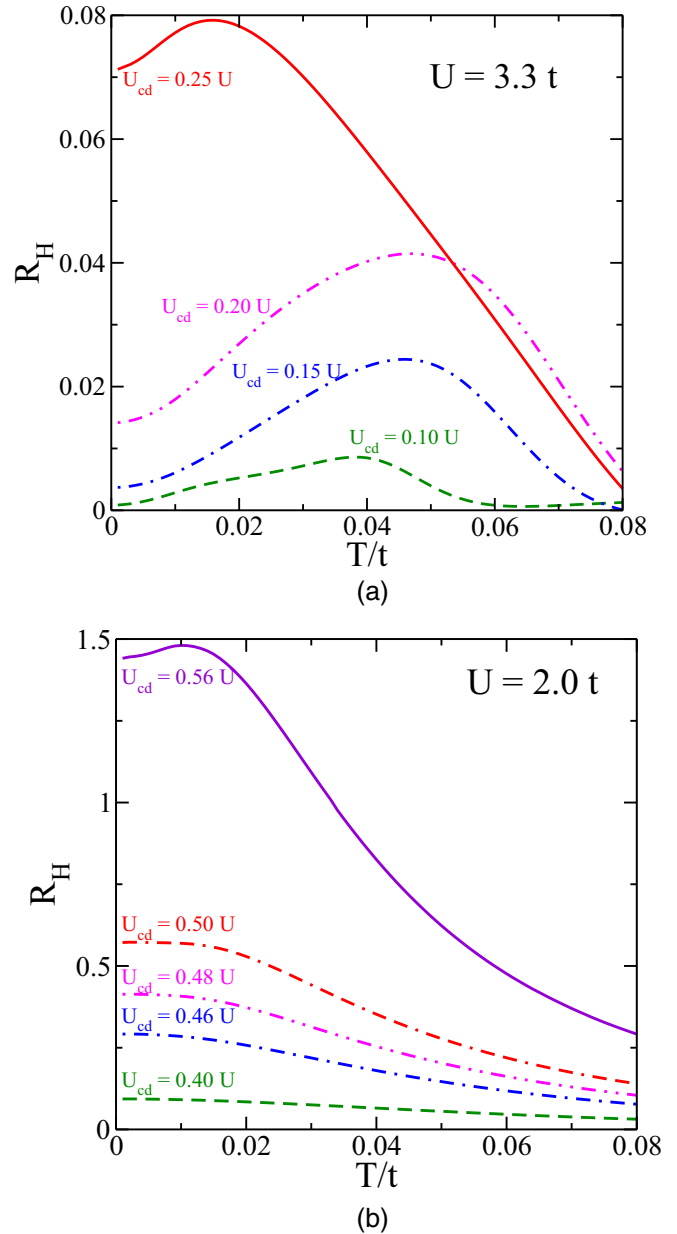


FIG. 3. Hall coefficient (R_H) vs temperature plot at (a) $U = 3.3t$ and (b) $U = 2.0t$. Dashed lines are power-law fits at low T .

even as the exponent α continuously varies between 1.0 and 2.0. Our results are completely consistent with data for $V_{2-y}O_3$ in all respects: (i) specifically, $\rho_{dc}(T) \simeq \rho_0(y) + AT^\alpha$ with $1.5 \leq \alpha < 2$ in data agrees well with our estimate $1.2 \leq 1.76$ in the NFL regime of H^{HFKM} [3,4], (ii) $\cot \theta_H(T) = C_1 + C_2 T^2$ up to $T \simeq 500$ K upon choosing $t = 1.0$ eV in the model, again in nice accord with data [3]. (iii) Concomitantly, $R_H(T)$ exhibits a strong T dependence, increasing slowly at low T and forming a clear peak at high U_{cd} , and decreasing rapidly at T increases further [3]. Like found in the experiment, at U close to the Mott insulator and low U_{cd} , an upturn in $\cot \theta_H$ is noticed showing a $C_1 + (C_2 - C_3 T)^2$ dependence on T . This occurs because the Hall coefficient R_H 's peak changes position with U_{cd} at $U/t = 3.3$, which is close to the Mott MIT whereas away from the MIT ($U = 2t$) the peak is merely formed (in

fact R_H has a negligible T dependence at low U as can be expected for low U/t). Though in the $V_{2-y}O_3$ experiment in Ref. [3] the origin of the upturns due to HFKM physics remains inconclusive since the Néel phase almost commences after the turning point, our formalism at least offers a scenario where a deviation from strict $\cot\theta_H(T) = C_1 + C_2 T^2$ may occur. While more such experiments are demanded in correlated bulk materials, such upturns have been also noticed in several cuprate materials [26,27].

Thus, (magneto)transport responses in H^{HFKM} within DMFT exhibit comprehensive qualitative agreement with the complete set of data for $V_{2-y}O_3$. In particular, our results now strongly support the notion that emergence of two relaxation rates, or that the different decay rates for longitudinal and Hall currents, is a direct consequence of breakdown of the FL metal by strong scattering. As discussed above, the FK term in Eq. (1) can mimic either “intrinsic” scattering coming from selectively Mott localized states in a multiband system, or arising from strong “disorder” scattering. This is because correlations have already drastically renormalized the band energy scale to a much lower value associated with collective Kondo screening induced “heavy” FL. In such a situation, even modest disorder will appear “strong,” since the relevant scale that sets the relevance of disorder is now $U_{cd}n_i^d/k_B T_{\text{coh}}$ (with coherence temperature T_{coh} being small near the Mott transition) rather than $U_{cd}n_i^d/W$, with W , the free bandwidth for $U = 0$ bandwidth for $U = 0$.

IV. CHARGE-SPIN SEPARATION

The above observations call for a deeper understanding in terms of basic microscopic responses involving the interplay between the FK and onsite Hubbard interaction terms. Since DMFT is a self-consistently embedded impurity problem, and the anomalies are seen in the strongly correlated metallic state, we choose to tease out the deeper underlying reasons by analyzing the Wolff Falicov Kimball (WFKM) model as a simplified d -impurity model. The WFKM lacks the impurity-lattice hybridization compared to the actual Anderson impurity model, however, the Weiss Green’s retains the same form [18] and it is amenable to bosonization through a generalization of earlier attempts [28]. Such an analysis has the potential to bare the asymptotic separation of spin and charge modes, facilitating DMFT observation of two relaxation rates. Wolff impurity model including the FK coupling reads (see Appendix B for details)

$$H^{\text{WFKM}} = \sum_{k,\sigma} \tilde{\epsilon}_k c_{k\sigma}^\dagger c_{k\sigma} + U n_{0,d,\uparrow} n_{0,d,\downarrow} + U_{cd} \sum_{\sigma} n_{0,c,\sigma} n_{0,d} - \mu \sum_{\sigma} n_{0,c,\sigma}. \quad (2)$$

The WFKM for $U_{cd} = 0$ is bosonized as usual on a $(1 + 1)D$ half line and the result is a set of two independent gaussian models for *bosonic* spin (S) and charge (C) fluctuation modes emanating from the “impurity” (site 0) in each radial direction. The bosonized Hamiltonian is $H^{\text{WFKM}} = H_C + H_S$

where

$$H_C = \frac{v_F}{2} \int dy [\Pi_C^2(y) + (\partial_y \phi_C)^2] + \frac{(U n_0 - \mu + U_{cd} \bar{n}^d)}{\sqrt{2}\pi} [\partial_y \Phi_C(0)] + \frac{U}{8\pi^2} [\partial_y \Phi_C(0)]^2, \quad (3)$$

$$H_S = \frac{v_F}{2} \int dy [\Pi_S^2(y) + (\partial_y \phi_S)^2] - \frac{U}{8\pi^2} [\partial_y \Phi_S(0)]^2 \quad (4)$$

for a nonmagnetic ground state, where $\phi_v(y)$ and $\Pi_v(y)$ ($v = C, S$) are conjugate bosonic fields: $\Phi_v(y) = \sqrt{\pi}[\phi_v(y) - \int_{-\infty}^y dy' \Pi_v(y')]$, v_F is the Fermi velocity, n_0 and \bar{n}^d correspond to the occupation of noninteracting c fermions and average occupation of the d electron over a disorder distribution (i.e., effectively the disorder contribution x mentioned before). The FK term couples solely to the charge bosons, but with a subtlety that would result in interesting anomalies. Viewed at the basic scattering level, $U_{cd} \sum_i n_{ic} \langle \hat{n}_i^d \rangle$ acts as a strong scattering potential. Since $[\hat{n}_i^d, H] = 0 \forall i$ in the HFKM, $n_i^d = \langle \hat{n}_i^d \rangle = 0, 1$ and, viewed by a propagating c fermion, $U_{cd} \langle n_i^d \rangle$ now represents a “suddenly switched on” scattering potential that successively switches suddenly between 0 and U_{cd} . In the local impurity problem, this is thus precisely the famed x-ray edge (XRE) problem [29,30] (U_{cd} is the precise analog of the suddenly switched-on “core-hole” potential) in the charge channel; the spin channel is left unaffected.

Explicitly, expanding the charge-bosonic field in Fourier components, $\phi_C(x) = \sum_k (\sqrt{2|k|})^{-1} (a_k e^{ikx} + a_k^\dagger e^{-ikx}) e^{-\alpha|k|/2}$ and $\Pi_C(x) = -i \sum_k \sqrt{|k|/2} (a_k e^{ikx} - a_k^\dagger e^{-ikx}) e^{-\alpha|k|/2}$ (α is ultraviolet cutoff), one gets

$$H_C = \sum_{k>0} \omega_k a_k^\dagger a_k + i\sqrt{2\rho}(U n_0 - \mu + U_{cd} \bar{n}^d) \sum_{k>0} \sqrt{\omega_k} (a_k - a_{-k}) - \frac{\rho U}{2} \sum_{k,k'>0} (a_k - a_{-k})(a_{k'} - a_{-k'}), \quad (5)$$

where $a_k^\dagger = a_{-k}$, $\rho = (2\pi v_F)^{-1}$, $\omega_k = k v_F$. Thus H_C now corresponds to a Luttinger-Tomonaga model with shifted oscillator modes $b_k \equiv a_k - i(U n_0 - \mu + U_{cd} \langle n^d \rangle)/(v_F \sqrt{k})$ (see Appendix B). The effect of this shift has an important consequence, namely the time-dependent Green’s function vanishes as a power law at large time $G(t) \propto t^{-(\delta/\pi)^2}$ where $\delta/\pi = D_0(\mu) U_{cd}$, D_0 being the noninteracting density of states (DoS) [30–34] in the s -wave scattering approximation. This interesting phenomenon is famously known as the Anderson’s *orthogonality catastrophe* (OC), where he showed that the quantum fidelity or overlap between the wave functions with and without the core potential in the XRE problem vanishes at the thermodynamic limit [35]. Reference [14] showed that the XRE problem can be mapped to the FKM since both share the same solution for the c -electron Green’s function.

Anderson offered a *tomographic* Luttinger liquid theory (TLT) in order to explain the two different relaxation rates found in the longitudinal and transverse transport properties

of cuprate superconductors [2]. There he adopted the idea of spin-charge separation based on the bosonization method by Luther for higher dimension [36]. Following the TLLT an external electric field accelerates charge, leading to a spinon backflow, and induces scattering between spin and charge. In $D = 3$, one expects that scattering off local, dynamical spin fluctuations will lead to the dc resistivity $\rho_{dc}(T) \simeq T^{D/2} = T^{3/2}$. However, an external magnetic field will couple solely to the spin modes (equivalently spin fermions or “spinons” as above), leading to a Hall relaxation rate entirely determined by “spinon-spinon” scattering, giving $\cot\theta_H \simeq \tau_H^{-1} = C_2 T^2$. In the presence of additional strong scattering due to either an intrinsically localized electronic (U_{cd}) or disorder channel, there will generically be a term $\tau_H^{-1} \simeq C_1$ in addition to the above, yielding $\cot\theta_H \simeq C_1 + C_2 T^2$. On the other hand, since the charge fluctuations are directly affected thereby, the resulting modification of scattering processes involving charge and spin modes can lead to deviation from the $\rho_{dc}(T) \simeq T^{3/2}$ in addition to contributing a residual ρ_0 term.

V. CONCLUSION

The finding of two relaxation rates for decay of longitudinal and Hall currents can now be rationalized by observing that these are consequences of the breakdown of FL concepts in the barely (bad) metallic state close to the Mott transition. Extinction of FL quasiparticles is associated with a “lattice” OC, which now occurs due to either a FK interaction [14] or strong disorder [37] in a metal already close to a correlation-driven Mott transition. In this context, it is interesting to observe that the hidden FL [38] also involves a related x-ray edge mechanism (at $U = \infty$) for destruction of FL theory. In our case, given finite $U \simeq W$ (the one-electron bandwidth), additional intrinsic or extrinsic disorder scattering channels are necessary to generate such a breakdown of FL theory.

It is worth mentioning the recent work on two-dimensional electron gases (2DEGs) formed at the interface between band and Mott insulators ($\text{SrTiO}_3/\text{RTiO}_3$, $R = \text{Gd, Sm}$) also reveal this striking two-relaxation rate scenario [39]. Further, this seems to be seen in various cases, irrespective of the nature of incipient magnetic ordering, degree of disorder, or emergence of NFL metallicity, pointing to its link to a deeper common underlying element. If we apply the above theory to 2DEGs like the above, the two-relaxation rates can arise from (i) a combination of electronic correlations plus atomic scale disorder at the interface, or (ii) in view of the multiband nature of quantum-well states (QWS) due to confinement effects, wherein interactions could selectively localize a subset of the QWS. Both these effects would give rise to a model akin to our Eq. (1), providing a rationale for these findings. It would be interesting to inquire whether a QCP associated with partial Mott selectivity (i.e., with an orbital-selective Mott phase) and/or disorder is implicated in samples which exhibit two-relaxation rates in (magneto)transport. That an effective mass divergence, rather than a Lifshitz transition, is implicated in this phenomenon [39] strongly hints at such a link, but more work is needed to establish it.

To summarize, we have investigated the emergence of two relaxation rates in correlated metals close to the Mott transition effectively in $D = 3$. We find that this unique feature is tied

to the loss of FL metallicity in symmetry-unbroken metallic states proximate to Mott transition(s): This can arise from strong scattering processes either stemming from intrinsic, (selectively-Mott) localized electrons, or from disorder which is generically relevant near a MIT. It is thus not specific to low dimensions. Surprisingly, comparison with data [3] for V_{2-y}O_3 reveals very good qualitative accord with all unusual features: (i) $\rho_{dc} \simeq \rho_0(y) + AT^{\alpha(y)}$ with $1.2 \leq \alpha \leq 1.6$, (ii) a strong T -dependent Hall constant, peaking at low T , and (iii) much less “unaffected by disorder-induced scattering” behavior of $\cot\theta_H(T) \simeq C_1 + C_2 T^2$.

ACKNOWLEDGMENT

We are thankful to the Department of Atomic Energy (DAE), Govt. of India for financial support.

APPENDIX A: DMFT METHOD

1. Formulation

In the DMFT method, we solve the effective quantum impurity model by the iterated perturbation theory (IPT), which is the second order self-energy approximation around the Hartree-Fock (HF) term [18,19]

$$\Sigma(\omega) = \Sigma_{\text{HF}} + \Sigma^{(2)}(\omega) \quad (\text{A1})$$

with

$$\Sigma_{\text{HF}} = U \langle \hat{n}_\sigma \rangle = Un/2; \quad (\text{A2})$$

$$\Sigma^{(2)}(\omega) = \lim_{i\omega_n \rightarrow \omega} \frac{U^2}{\beta^2} \sum_{m,p} \mathcal{G}(i\omega_n + i\nu_m) \mathcal{G}(i\omega_p + i\nu_m) \mathcal{G}(i\omega_p), \quad (\text{A3})$$

where \mathcal{G} is the propagator for the noninteracting electrons ($U = 0$) connected to the impurity site through a hybridization function $\Delta(\omega) : \mathcal{G}(\omega) = 1/(\omega + \mu - \Delta(\omega))$, μ being the chemical potential. Since $\Delta(\omega)$ is unknown, we determine \mathcal{G} through the Dyson equation once we evaluate the local Green’s function for a given lattice (steps are discussed below).

U_{cd} , in Eq. (1) of the main text, is treated as the site-disorder potential v through the coherent potential approximation (CPA), given a disorder concentration x at half filling [22] ($n = 1$). The DMFT+IPT+CPA approach takes the following steps.

Step 1. Evaluate $\Sigma_{\text{IPT}}(\omega)$ using Eqs. (A1)–(A3). In the first iteration, since no information about \mathcal{G} is available, we start with a guess self-energy (typically $\Sigma_{\text{guess}} = \Sigma_{\text{HF}}$).

Step 2. Using the noninteracting density of states (DoS) D_0 , find the local Green’s function:

$$\begin{aligned} G(\omega) &= \sum_{\mathbf{k}} \frac{1}{\omega^+ + \mu - \epsilon_{\mathbf{k}} - \Sigma(\omega)} \\ &= \int_{-\infty}^{\infty} d\epsilon \frac{D_0(\epsilon)}{\omega^+ + \mu - \epsilon - \Sigma(\omega)}. \end{aligned} \quad (\text{A4})$$

Step 3. For iteration number > 1 , check convergence in $G(\omega)$. Typically, convergence $C = -\text{Im} \int d\omega (G_{\text{now}} - G_{\text{previous}})$. Stop if $|C| < \eta$ where η is a tolerance factor (typically 10^{-4} or 10^{-5}) or else proceed to Step 4.

Step 4. Find the CPA self-energy and Green's function for a given disorder concentration x :

$$\Sigma_{\text{CPA}}(\omega) = xv + \frac{x(1-x)v^2}{\omega - v(1-x) - \Delta(\omega)}, \quad (\text{A5})$$

$$\mathcal{G}_{\text{CPA}}(\omega) = \frac{1-x}{\omega - \Delta(\omega)} + \frac{x}{\omega - v - \Delta(\omega)}, \quad (\text{A6})$$

where the Dyson equation gives $\Delta(\omega) = \omega + \mu - v/2 - \Sigma(\omega) - G^{-1}(\omega)$, $\Sigma(\omega) = \Sigma_{\text{IPT}} + \Sigma_{\text{CPA}}$ being the total self-energy.

Step 5. Assign $\mathcal{G} = \mathcal{G}_{\text{CPA}}$ and go back to *Step 1* and repeat consecutive steps.

Note that at the half filling the chemical potential is determined from $\mu = (U + v)/2$. Away from half filling one needs to apply the generalized IPT ansatz and employ the Luttinger theorem to determine μ in the metallic phase at zero temperature [40].

In order to find the transport properties we use the transport functions Φ_{xx} and Φ_{xy} for dc conductivity and Hall conductivity, respectively [25,41–44]:

$$\sigma_{xx} = c_{xx} \int_{-\infty}^{\infty} d\omega \frac{-\partial f(\omega)}{\partial \omega} \int_{-\infty}^{\infty} d\epsilon \Phi_{xx}(\epsilon) A(\omega, \epsilon)^2; \quad (\text{A7})$$

$$\sigma_{xy} = c_{xy} B \int_{-\infty}^{\infty} d\omega \frac{-\partial f(\omega)}{\partial \omega} \int_{-\infty}^{\infty} d\epsilon \Phi_{xy}(\epsilon) A(\omega, \epsilon)^3 \quad (\text{A8})$$

where $A(\omega, \epsilon) = -\text{Im}G(\omega, \epsilon_{\mathbf{k}} = \epsilon)/\pi$; $c_{xx} = e^2\pi/(2\hbar a)$ (e : electron's charge, a : lattice constant); $c_{xy} = 2e^3\pi^2 a/(3\hbar^2)$; B is the external magnetic field in a Hall experiment, and the transport functions are [25]

$$\begin{aligned} \Phi_{xx}(\epsilon) &= \frac{1}{4d} D_0(\epsilon), \\ \Phi_{xy}(\epsilon) &= -\frac{1}{4d^2} \epsilon D_0(\epsilon) \end{aligned} \quad (\text{A9})$$

with d being the dimension and $D_0(\epsilon) = 2/(\pi t) \sqrt{1 - (\epsilon/t)^2}$ being the noninteracting density of states (DoS) for the Bethe lattice used in our model.

The Hall coefficient (R_H) and cotangent of Hall angle θ_H are found from Eqs. (A7) and (A8):

$$R_H = \sigma_{xy}/(\sigma_{xx}^2 B), \quad (\text{A10})$$

$$\cot \theta_H = \sigma_{xx}/\sigma_{xy}. \quad (\text{A11})$$

In our work, we select the hopping amplitude $t = 1$ and also set $c_{xx} = c_{xy} = B = d = 1$.

2. Spectral density and self-energy

At $U_{cd} = 0$ and low interaction strength ($U/t < U_{c2}/t$), a clear quasiparticle resonance in spectral density appears at the Fermi level ($\omega = \mu = 0$). As soon as U_{cd} is turned on, the height of the resonance starts diminishing and spectral density gets broadened (see Figure 4). After a certain threshold value of $U_{cd}^{\text{th}} (\simeq 0.35U$ at $U = 2.0t$ and disorder concentration $x = 0.45$) the peak melts down to a dip and Landau's Fermi liquid

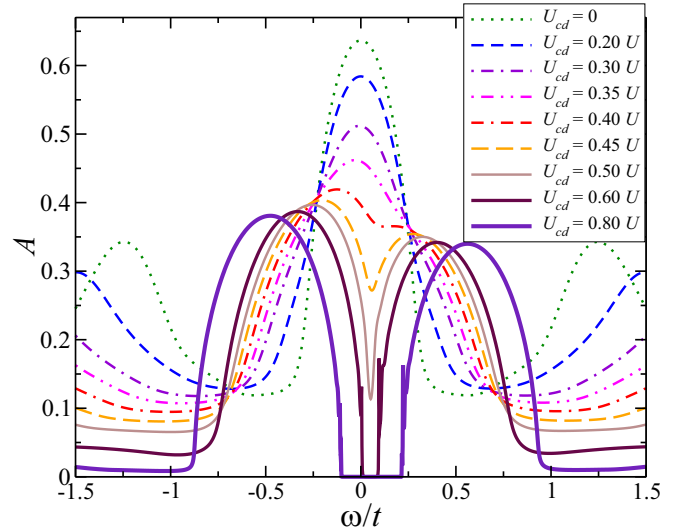


FIG. 4. Spectral density $A(\omega/t)$ at various U_{cd} 's for $U = 2.0t$ and $x = 0.45$. Finite U_{cd} leads to depletion of the height of the quasiparticle resonance by broadening it around the Fermi level ($\omega = 0$). At $U_{cd} > 0.35U$, the resonance starts disappearing by forming a dip or *pseudogap* near the Fermi level.

(FL) quasiparticle picture no longer sustains. Further increase of U_{cd} enhances the depth of the dip which finally opens a gap at the Fermi level at $U_{cd} = U_{cd}^{\text{crit}} (\simeq 0.60U$ for $x = 0.45$, $U = 2.0t$) indicating a metal-to-insulator (MIT) transition. This result qualitatively agrees with earlier calculations with other methods and cluster variations [20,23,45–48].

The destruction of the quasiparticle and hence FL at $U_{cd} > U_{cd}^{\text{th}}$ is evident from the imaginary part of the self-energy $\Sigma(\omega)$. $\text{Im}\Sigma(\omega)$ follows $A + B\omega^2$ behavior at very low U_{cd} in the vicinity of $\omega = 0$ ($A = 0$ when $U_{cd} = 0$). As U_{cd} is increased, $\text{Im}\Sigma$'s quadratic dependence on ω wears off and instead a peaklike structure arises near the Fermi level, again signifying a transition from coherent to incoherent metal. In the coherent regime the quasiparticle residue $Z \equiv [1 - \partial \text{Re}\Sigma(\omega)/\partial \omega]_{\omega=0}^{-1}$ increases with U_{cd} and in the incoherent regime it loses any physical meaning [22] (see Figure 5). It is intuitive and evident from Figure 4 that U_{cd} competes against the onsite Coulomb interaction U as the former broadens the quasiparticle resonance whereas the latter shrinks it in the FL regime. Such broadening effectively enhances the quasiparticle lifetime and hence Z increases with $U_{cd} \leq U_{cd}^{\text{th}}$, as already shown in the inset of Figure 5. However, since disorder also piles up the incoherent scattering, $U_{cd} > U_{cd}^{\text{th}}$ eventually leads to an insulating gap in the spectral density even though the clean system ($U_{cd} = 0$ case) is metallic. Therefore increasing onsite interaction U encourages coherent-to-incoherent metal transition to occur sooner and hence U_{cd}^{th} and U_{cd}^{crit} diminishes. Figure 6 approves the same plot for $x = 0.5$.

APPENDIX B: BOSONIZATION METHOD

Here we present some details of the bosonization approach used in the main text.

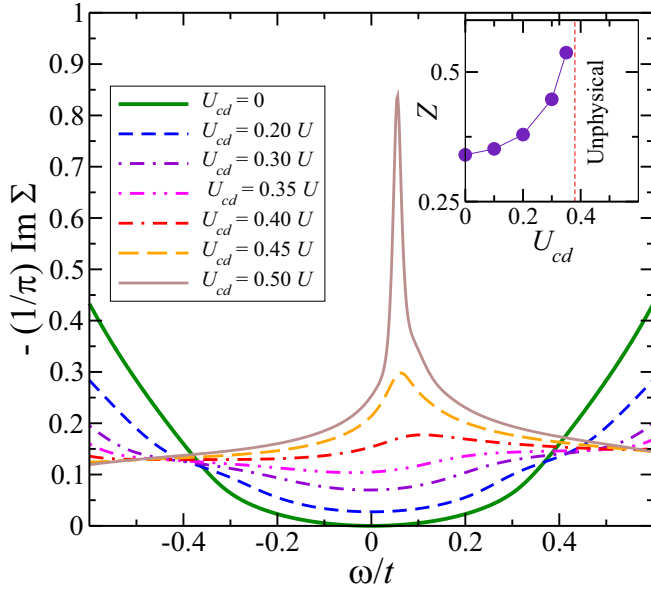


FIG. 5. Imaginary part of self-energy plotted (with $-1/\pi$ factor) as functions of ω at various U_{cd} 's at $U = 2.0t$ and $x = 0.45$. For low U_{cd} , $\text{Im}\Sigma(\omega)$ behaves FL-like: $\text{Im}\Sigma(\omega \rightarrow 0) = A + B\omega^2$ ($A = 0$ at $U_{cd} = 0$). However, for $U_{cd} = U_{cd}^{\text{th}} \simeq 0.35U$, FL starts developing a peak near the Fermi level signifying incoherent or bad metallic behavior. The inset shows that quasiparticle residue Z increases as U_{cd} is enhanced up to U_{cd}^{th} , beyond that Z becomes meaningless or unphysical.

1. Wolff model

The Wolff model bears the same relation to the lattice Hubbard model as the Anderson impurity model bears to the periodic Anderson model. It describes a band of conduction electrons (dispersion denoted by $\tilde{\epsilon}_k$) interacting only at site-0 via a Hubbard term

$$H^W = \sum_{k,\sigma} \tilde{\epsilon}_k c_{k\sigma}^\dagger c_{k\sigma} + U n_{0\uparrow} n_{0\downarrow} - \mu \sum_{\sigma} n_{0\sigma}. \quad (\text{B1})$$

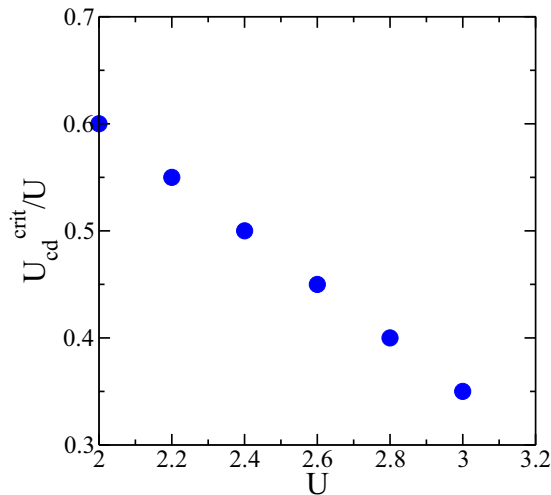


FIG. 6. U_{cd}^{crit} vs U for $x = 0.5$.

This impurity model can also be recast as

$$H^W = \sum_{\sigma} \left[i v_F \int_{-\infty}^{\infty} dy \Psi_{\sigma}^{\dagger}(y) \partial_y \Psi_{\sigma}(y) + \frac{U}{2} : \Psi_{\sigma}^{\dagger}(0) \Psi_{\sigma}(0) :: \Psi_{\bar{\sigma}(0)}^{\dagger} \Psi_{\bar{\sigma}(0)} : - \mu : \Psi_{\sigma}^{\dagger}(0) \Psi_{\sigma}(0) : \right], \quad (\text{B2})$$

where the radial motion of the band electrons is described by chiral (right movers) real space fermion fields $\Psi_{\sigma}(y)$, $v_F = \partial_k \tilde{\epsilon}_k|_{k=k_F}$, $\bar{\sigma} = -\sigma$ and $:$ \hat{A} $:$ implies the normal ordering of \hat{A} ($:$ $\hat{A} := \hat{A} - \langle 0|\hat{A}|0\rangle$; $|0\rangle$ is the ground state). We want to use the standard bosonization identity

$$\Psi_{\sigma}(y) = \frac{1}{\sqrt{2\pi\alpha}} e^{i\Phi_{\sigma}(y)}; \quad \Phi_{\sigma}(y) = \sqrt{\pi} \left[\phi_{\sigma}(y) - \int_{-\infty}^y dy' \Pi_{\sigma}(y') \right], \quad (\text{B3})$$

where $\phi_{\sigma}(y)$ and $\Pi(y)$ are the conjugate bosonic fields satisfying the commutation $[\phi_{\sigma}(y), \Pi_{\sigma'}(y')] = i\delta_{\sigma\sigma'}\delta(y - y')$ and α is the ultraviolet cutoff [49].

Now we introduce the charge and spin field as

$$\Phi_C = \sum_{\sigma} \Phi_{\sigma}; \quad \Phi_S = \sum_{\sigma} \sigma \Phi_{\sigma} \quad (\text{B4})$$

and break the Hamiltonian into charge (C) plus spin (S) parts:

$$H^W = H_C^W + H_S^W \quad (\text{B5})$$

with

$$H_C^W = \frac{v_F}{2} \int_{-\infty}^{\infty} dy [\Pi_C^2(y) + (\partial_y \phi_C(y))^2] - \frac{U n_0 - \mu}{\sqrt{2\pi}} \partial_y \Phi_C(0) + \frac{U}{8\pi^2} (\partial_y \Phi_C(0))^2, \quad (\text{B6})$$

$$H_S^W = \frac{v_F}{2} \int_{-\infty}^{\infty} dy [\Pi_S^2(y) + (\partial_y \phi_S(y))^2] - \frac{U}{\sqrt{2\pi}} (\partial_y \Phi_S(0))^2 - \frac{U}{8\pi^2} (\partial_y \Phi_S(0))^2, \quad (\text{B7})$$

$$: \Psi_{\sigma}^{\dagger}(0) \Psi_{\sigma}(0) : = \frac{1}{2\pi} \partial_y \Phi_{\sigma}(0), \quad (\text{B8})$$

and

$$n_0 = \langle \Psi_{\sigma}^{\dagger}(0) \Psi_{\sigma}(0) \rangle_{U=0} \quad (\text{B9})$$

consider as the ground state occupancy. Now once we resolve the bosonic field operators into their Fourier components, i.e.,

$$\phi_v(y) = \sum_k \frac{1}{\sqrt{2|k|}} (a_{v,k} e^{iky} + a_{v,k}^{\dagger} e^{-iky}) e^{-\alpha|k|/2}, \quad (\text{B10})$$

$$\Pi_v(y) = -i \sum_k \sqrt{\frac{|k|}{2}} (a_{v,k} e^{iky} - a_{v,k}^{\dagger} e^{-iky}) e^{-\alpha|k|/2} \quad (\text{B11})$$

(where $v = C, S$), we reexpress the Hamiltonians in terms of momentum based bosonic operators $a_{v,k}$:

$$H_C^W = \sum_{k>0} \omega_k a_{C,k}^\dagger a_{C,k} + i\sqrt{2\rho}(Un_0 - \mu) \sum_{k>0} \sqrt{\omega_k}(a_{C,k} - a_{C,k}^\dagger) - \frac{\rho U}{2} \sum_{k,k'>0} (a_{C,k} - a_{C,k}^\dagger)(a_{C,k'} - a_{C,k'}^\dagger) \quad (B12)$$

$$H_S^W = \sum_{k>0} \omega_k a_{S,k}^\dagger a_{S,k} + \frac{\rho U}{2} \sum_{k,k'>0} \sqrt{\omega_k \omega_{k'}} \times (a_{S,k} - a_{C,k}^\dagger)(a_{S,k'} - a_{S,k'}^\dagger), \quad (B13)$$

where $\omega_k \equiv kv_F$ and $\rho \equiv 1/(2\pi v_F)$.

Now within this formalism, it may not be straightforward to find the finite temperature transport properties and capture their distinct behaviors arising from H_C and H_S . However, for a simple demonstration, one can show that zero temperature response functions behave differently, particularly adopting the equation of motion method and taking the zero frequency limit [50], one can show that the local charge susceptibility:

$$\chi_C = \frac{1}{\rho(U_C + U)} \quad (B14)$$

and the local spin susceptibility:

$$\chi_S = \frac{1}{\rho(U_C - U)} \quad (B15)$$

with $U_C \equiv 2\rho^2$. Clearly χ_S is enhanced with increasing U while χ_C is suppressed.

2. Effect of Falicov-Kimball interaction

The WFKM in Eq. (2) of the main text is written in the impurity limit by separating the FK term

$$H^{\text{HFKM}} = H^W + U_{cd} \int dy \sum_\sigma : \Psi_\sigma^\dagger(0) \Psi_\sigma(0) : n^d(y). \quad (B16)$$

Upon bosonization, we find that the d electrons couple only to the charge sector

$$H_C^{\text{WFKM}} = \frac{v_F}{2} \int_{-\infty}^{\infty} dy [\Pi_C^2(y) + (\partial_y \phi_C(y))^2] - \frac{U/2 - \mu + U_{cd}\bar{n}^d}{\sqrt{2\pi}} \partial_x \Phi_C(0) + \frac{U}{8\pi^2} (\partial_y \Phi_C(0))^2, \quad (B17)$$

$$H_S^{\text{WFKM}} = \frac{v_F}{2} \int_{-\infty}^{\infty} dy [\Pi_S + (\partial_y \phi_C(y))^2] - \frac{U}{\sqrt{2\pi}} (\partial_y \Phi_S(0))^2 - \frac{U}{8\pi^2} (\partial_y \Phi_S(0))^2, \quad (B18)$$

where \bar{n}^d is the average d occupancy that depends on the disorder distribution (x in DMFT+CPA context).

Similar expressions have been found by Brydon and Gulácsi [51] for the Falicov-Kimball model while they considered spinful d electrons and Klein operators. As evident from Eq. (B18), the spin sector, however, does not experience U_{cd} , and continues to exhibit characteristics of the Wolff model [where $U_{cd} = 0$; cf. Eq. (B15)].

Again in a similar fashion, the Hamiltonians in momentum-space representation will be

$$H_C^{\text{WFKM}} = \sum_{k>0} \omega_k a_{C,k}^\dagger a_{C,k} + i\sqrt{2\rho}(Un_0 - \mu + U_{cd}\bar{n}^d) \times \sum_{k>0} \sqrt{\omega_k}(a_{C,k} - a_{C,k}^\dagger) - \frac{\rho U}{2} \sum_{k,k'>0} (a_{C,k} - a_{C,k}^\dagger)(a_{C,k'} - a_{C,k'}^\dagger) \quad (B19)$$

$$H_S^{\text{WFKM}} = \sum_{k>0} \omega_k a_{S,k}^\dagger a_{S,k} + \frac{\rho U}{2} \sum_{k,k'>0} \sqrt{\omega_k \omega_{k'}} (a_{S,k} - a_{S,k}^\dagger) \times (a_{S,k'} - a_{S,k'}^\dagger). \quad (B20)$$

Here the terms that appear in the form $A(k)a_{v,k}^\dagger a_{v,k} + iB(k)(a_{v,k} - a_{v,k}^\dagger) + C(k)$ can be easily rearranged as $A(k)b_{v,k}^\dagger b_{v,k} - B^2(k)/A(k)$; $b_{v,k} \equiv a_{v,k} - iB(k)/A(k) = a_{v,k} - i(Un_0 - \mu + U_{cd}\bar{n}^d)/(v_F\sqrt{k})$, which is nothing but a Tomonaga-Luttinger model with shifted oscillator modes, as first demonstrated by Schotte and Schotte in order to solve the x-ray edge problem [31]. The shift $iB(k)/A(k)$ clearly depends on the strength of FK interaction. The form $C(k,k')(a_{v,k} - a_{v,k}^\dagger)(a_{v,k'} - a_{v,k'}^\dagger)$ in the last term becomes $C(k,k')(b_{v,k} - b_{v,k}^\dagger)(b_{v,k'} - b_{v,k'}^\dagger)$.

Thus we see that the high-dimension spin-charge separation addressed to the main text arises because U_{cd} shifts the charge bosonic modes [cf. Eq. (B17)] but does not affect the spin bosons. Thus, the charge fluctuation modes develop low-energy incoherent structure due to an ‘‘orthogonality catastrophe’’ due to the sudden switching on of the FK potential (U_{cd}), while the spin fluctuation modes continue to exhibit an infrared polelike structure. One may say that the *holons*, viewed as emergent, collective charge fluctuation modes have a branch-cut propagator, while the *spinons*, viewed as emergent, collective spin fluctuation modes, have a pole in the associated propagator.

- [1] T. R. Chien, Z. Z. Wang, and N. P. Ong, *Phys. Rev. Lett.* **67**, 2088 (1991).
- [2] P. W. Anderson, *Phys. Rev. Lett.* **67**, 2092 (1991).
- [3] T. F. Rosenbaum, A. Husmann, S. A. Carter, and J. M. Honig, *Phys. Rev. B* **57**, R13997 (1998).

- [4] S. Klimm, M. Herz, R. Horny, G. Obermeier, M. Klemm, and S. Horn, *J. Magn. Magn. Mater.* **226**, 216 (2001).
- [5] M. S. Laad, I. Bradarić, and F. V. Kusmartsev, *Phys. Rev. Lett.* **100**, 096402 (2008).

- [6] Y. A. Ying, Y. Liu, T. He, and R. J. Cava, *Phys. Rev. B* **84**, 233104 (2011).
- [7] S. Nair, S. Wirth, S. Friedemann, F. Steglich, Q. Si, and A. J. Schofield, *Adv. Phys.* **61**, 583 (2012).
- [8] S. A. Carter, J. Yang, T. F. Rosenbaum, J. Spalek, and J. M. Honig, *Phys. Rev. B* **43**, 607 (1991).
- [9] P. Werner, S. Hoshino, and H. Shinaoka, *Phys. Rev. B* **94**, 245134 (2016).
- [10] M. S. Laad, L. Craco, and E. Müller-Hartmann, *Phys. Rev. Lett.* **91**, 156402 (2003).
- [11] M. S. Laad, L. Craco, and E. Müller-Hartmann, *Phys. Rev. B* **73**, 045109 (2006).
- [12] K. Held, G. Keller, V. Eyert, D. Vollhardt, and V. I. Anisimov, *Phys. Rev. Lett.* **86**, 5345 (2001).
- [13] A. I. Poteryaev, J. M. Tomczak, S. Biermann, A. Georges, A. I. Lichtenstein, A. N. Rubtsov, T. Saha-Dasgupta, and O. K. Andersen, *Phys. Rev. B* **76**, 085127 (2007).
- [14] Q. Si, G. Kotliar, and A. Georges, *Phys. Rev. B* **46**, 1261 (1992).
- [15] J. K. Freericks and V. Zlatić, *Rev. Mod. Phys.* **75**, 1333 (2003).
- [16] L. de'Medici, A. Georges, and S. Biermann, *Phys. Rev. B* **72**, 205124 (2005).
- [17] S. Biermann, L. de'Medici, and A. Georges, *Phys. Rev. Lett.* **95**, 206401 (2005).
- [18] A. Georges, G. Kotliar, W. Krauth, and M. J. Rozenberg, *Rev. Mod. Phys.* **68**, 13 (1996).
- [19] H. Barman and N. S. Vidhyadhiraja, *Int. J. Mod. Phys. B* **25**, 2461 (2011).
- [20] C. E. Ekuma, S.-X. Yang, H. Terletska, K.-M. Tam, N. S. Vidhyadhiraja, J. Moreno, and M. Jarrell, *Phys. Rev. B* **92**, 201114 (2015).
- [21] N. Dasari, W. R. Mondal, P. Zhang, J. Moreno, M. Jarrell, and N. S. Vidhyadhiraja, *Eur. Phys. J. B* **89**, 202 (2016).
- [22] M. S. Laad, L. Craco, and E. Müller-Hartmann, *Phys. Rev. B* **64**, 195114 (2001).
- [23] M. M. Radonjić, D. Tanasković, V. Dobrosavljević, and K. Haule, *Phys. Rev. B* **81**, 075118 (2010).
- [24] A. I. Poteryaev, S. L. Skornyakov, A. S. Belozarov, and V. I. Anisimov, *Phys. Rev. B* **91**, 195141 (2015).
- [25] E. Lange and G. Kotliar, *Phys. Rev. B* **59**, 1800 (1999).
- [26] Y. Abe, K. Segawa, and Y. Ando, *Phys. Rev. B* **60**, R15055 (1999).
- [27] K. Segawa and Y. Ando, *Phys. Rev. B* **69**, 104521 (2004).
- [28] G.-M. Zhang, Z.-B. Su, and L. Yu, *Phys. Rev. B* **49**, 7759 (1994).
- [29] G. D. Mahan, *Phys. Rev.* **163**, 612 (1967).
- [30] P. Nozières and C. T. de Dominicis, *Phys. Rev.* **178**, 1097 (1969).
- [31] K. D. Schotte and U. Schotte, *Phys. Rev.* **185**, 509 (1969).
- [32] S. Doniach and M. Sunjic, *J. Phys. C* **3**, 285 (1970).
- [33] D. R. Hamann, *Phys. Rev. Lett.* **26**, 1030 (1971).
- [34] E. Müller-Hartmann, T. V. Ramakrishnan, and G. Toulouse, *Phys. Rev. B* **3**, 1102 (1971).
- [35] P. W. Anderson, *Phys. Rev. Lett.* **18**, 1049 (1967).
- [36] A. Luther, *Phys. Rev. B* **19**, 320 (1979).
- [37] B. L. Altshuler, A. G. Aronov, and D. E. Khmel'nitsky, *J. Phys. C* **15**, 7367 (1982).
- [38] P. W. Anderson, *Phys. Rev. B* **78**, 174505 (2008).
- [39] E. Mikhaylov, C. R. Freeze, B. J. Isaac, T. A. Cain, and S. Stemmer, *Phys. Rev. B* **91**, 165125 (2015).
- [40] H. Kajueter and G. Kotliar, *Phys. Rev. Lett.* **77**, 131 (1996).
- [41] P. Voruganti, A. Golubentsev, and S. John, *Phys. Rev. B* **45**, 13945 (1992).
- [42] T. Pruschke, M. Jarrell, and J. Freericks, *Adv. Phys.* **44**, 187 (1995).
- [43] P. Majumdar and H. R. Krishnamurthy, [arXiv:cond-mat/9512151](https://arxiv.org/abs/cond-mat/9512151).
- [44] P. Majumdar and H. R. Krishnamurthy, [arXiv:cond-mat/9604057](https://arxiv.org/abs/cond-mat/9604057).
- [45] K. Byczuk, W. Hofstetter, and D. Vollhardt, *Int. J. Mod. Phys. B* **24**, 1727 (2010).
- [46] D.-B. Nguyen and M.-T. Tran, *Phys. Rev. B* **87**, 045125 (2013).
- [47] D.-A. Le and M.-T. Tran, *Phys. Rev. B* **91**, 195144 (2015).
- [48] H. Lee, H. O. Jeschke, and R. Valentí, *Phys. Rev. B* **93**, 224203 (2016).
- [49] T. Giamarchi, *Quantum Physics in One Dimension*, The international series of monographs on physics 121 (Clarendon, Oxford University Press, Oxford, 2004).
- [50] Z. GuangMing, *Commun. Theor. Phys.* **34**, 211 (2000).
- [51] P. M. R. Brydon and M. Gulácsi, *Phys. Rev. B* **73**, 235120 (2006).